Cell Death &
Differentiation

ARTICLE

STAT3 localizes to the ER, acting as a gatekeeper for ER-mitochondrion Ca^{2+} fluxes and apoptotic responses

Lidia Avalle[1] · Annalisa Camporeale[1] · Giampaolo Morciano[2,3,4] · Natascia Caroccia[2] · Elena Ghetti[1] ·
Valeria Orecchia[1] · Daniele Viavattene[1] · Carlotta Giorgi[2] · Paolo Pinton [ID][2,3] · Valeria Poli [ID][1]

Abstract

STAT3 is an oncogenic transcription factor exerting its functions both as a canonical transcriptional activator and as a non-canonical regulator of energy metabolism and mitochondrial functions. While both activities are required for cell transformation downstream of different oncogenic stimuli, they rely on different post-translational activating events, namely phosphorylation on either Y705 (nuclear activities) or S727 (mitochondrial functions). Here, we report the discovery of the unexpected STAT3 localization to the endoplasmic reticulum (ER), from where it modulates ER-mitochondria Ca^{2+} release by interacting with the Ca^{2+} channel IP3R3 and facilitating its degradation. The release of Ca^{2+} is of paramount importance for life/death cell decisions, as excessive Ca^{2+} causes mitochondrial Ca^{2+} overload, the opening of the mitochondrial permeability transition pore, and the initiation of the intrinsic apoptotic program. Indeed, STAT3 silencing enhances ER Ca^{2+} release and sensitivity to apoptosis following oxidative stress in STAT3-dependent mammary tumor cells, correlating with increased IP3R3 levels. Accordingly, basal-like mammary tumors, which frequently display constitutively active STAT3, show an inverse correlation between IP3R3 and STAT3 protein levels. These results suggest that STAT3-mediated IP3R3 downregulation in the ER crucially contributes to its anti-apoptotic functions via modulation of Ca^{2+} fluxes.

Edited by E Gottlieb

These authors contributed equally: Lidia Avalle, Annalisa Camporeale, Giampaolo Morciano.

✉ Paolo Pinton
paolo.pinton@unife.it

✉ Valeria Poli
valeria.poli@unito.it

[1] Department of Molecular Biotechnology and Health Sciences, University of Torino, 10126 Torino, Italy

[2] Department of Morphology, Surgery and Experimental Medicine, University of Ferrara, 44121 Ferrara, Italy

[3] Cecilia Hospital, GVM Care & Research, 48033 Cotignola, Ravenna, Italy

[4] Maria Pia Hospital, GVM Care & Research, 10132 Torino, Italy

Introduction

Signal transducer and activator of transcription 3 (STAT3) is a pleiotropic transcription factor mediating the signaling of cytokines, growth factors, and oncogenes [1]. It becomes transcriptionally activated via phosphorylation on its Y705 residue, which allows productive dimerization, concentration into the nucleus, and DNA binding. STAT3 is able to activate a wide variety of target genes, modulating many cellular functions at both the physiological and pathological level. In particular, STAT3 is considered an oncogene in virtue of the observation that its constitutive activation is detected in many tumors of both solid and liquid origin, which often become addicted to its activity for growth and survival [1, 2]. This is corroborated by the detection of somatic activating mutations associated to cell transformation in inflammatory hepatocellular adenomas [3] and in hematological neoplasms [4]. Accordingly, STAT3 nuclear activity was shown to be required for cellular transformation downstream of several oncogenes that trigger its phosphorylation on Y705 (Y-P), the prototype being vSrc [5]. In tumors, STAT3 activity can drive survival, resistance to apoptosis and to chemotherapy, migration and invasion,
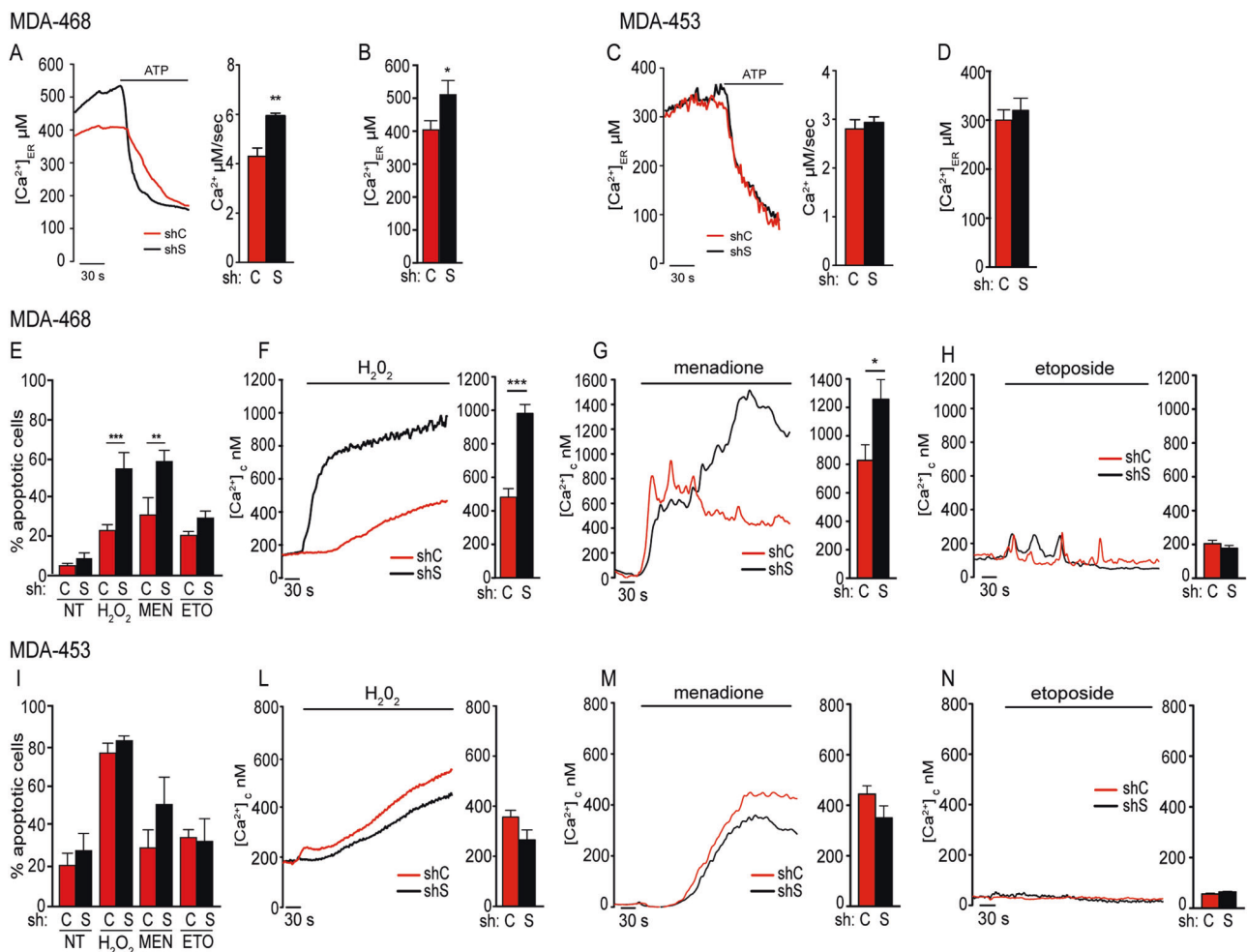
Fig. 1 Relevance of STAT3 in Ca²⁺ homeostasis and apoptotic response. MDA-MB-468 (**a**, **b**, **e–h**) or MDA-MB-453 cells (**c**, **d**, **i–n**), silenced or not for STAT3 (shS, shSTAT3; shC, sh control) were used as indicated. **a–d** ER Ca²⁺ content and release. To induce Ca²⁺ release from ER, the cells were challenged with ATP, which evokes a rapid discharge from inositol 1,4,5-phosphate receptors (IP3Rs). **a**, **c** Representative traces are shown. ER calcium release (mean ± SEM) is quantified by the bars and expressed as μM/s. **b**, **d** The steady-state Ca²⁺ content. Bars are mean ± SEM of at least eight traces from three independent experiments. **e**, **i** Apoptosis upon treatment with hydrogen peroxide (H₂O₂), menadione (MEN), or etoposide (ETO), measured by cytofluorimetry of Annexin V/PI⁺ cells in the indicated cells. Bars represent the percentage of Annexin V/PI-positive cells (mean ± SEM from five independent experiments). **f–h**, **l–n** Cytoplasmic Ca²⁺ release was measured upon the indicated treatments. Bars are mean ± SEM of 12 measurements from three independent experiments. The asterisks indicate statistically significant differences. *$P < 0.05$; **$P < 0.005$; ***$P < 0.001$

epithelial to mesenchymal transition, immune evasion and stemness [6]. Additionally, STAT3 can regulate energy metabolism, and its constitutive activation triggers a metabolic switch towards aerobic glycolysis, contributing to cell transformation and tumor cell survival [7, 8]. STAT3 can also be phosphorylated on S727 (S-P) downstream of both classical STAT3-activating pathways and of RAS proteins [9–11]. S-P is thought to mediate STAT3 non-canonical functions via localization to the mitochondria [10, 12]. Mitochondrial STAT3 is required to maintain the activity of the electron transfer complexes (ETC) under stress conditions or oncogenic transformation mediated by RAS oncogenes, while at the same time increasing aerobic glycolysis and decreasing ROS production, possibly by associating to

Complex I and by favoring the formation of respiratory supercomplexes [10, 12, 13]. Additionally, mitochondrial STAT3 participates in calcium (Ca²⁺) homeostasis by enhancing the uptake of Ca²⁺ by mitochondria and its release into the cytosol during IL-6-mediated T cell activation [13].

Ca²⁺ homeostasis plays a major role in regulating cellular energetics and life/death decisions [14], and the endoplasmic reticulum (ER) is the major intracellular Ca²⁺ storage compartment. Ca²⁺ release occurring at the apposition of ER and mitochondrial membranes, known as the mitochondrial-associated membranes (MAMs) [15], controls the entry of Ca²⁺ in the mitochondrial matrix [16]. The main effectors of the ER Ca²⁺ release pathway
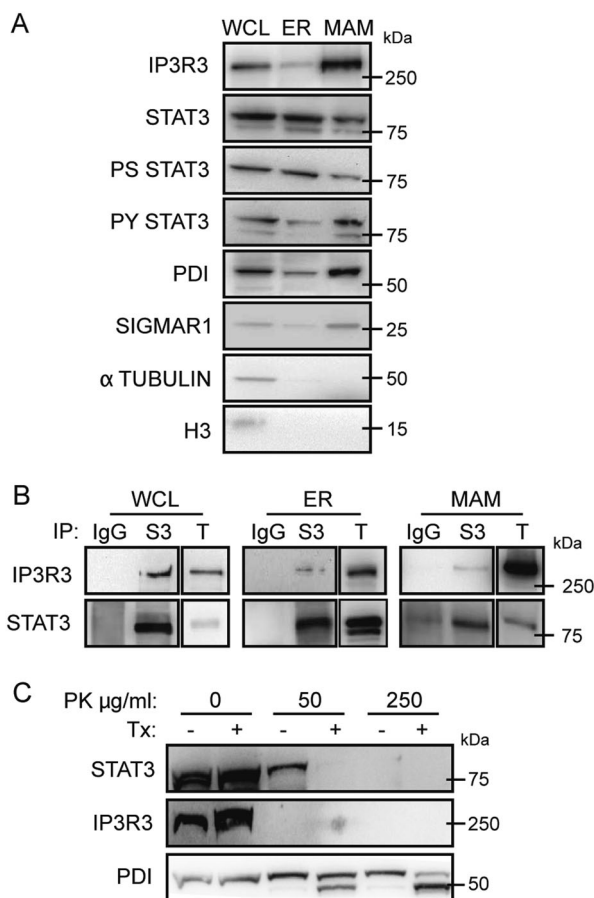
Fig. 2 STAT3 localizes to the ER and MAM compartments and interacts with IP3R3. **a** Whole-cell lysates from MDA-MB-468 cells were fractionated and analysed by Western blot. Representative of at least five independent experiments. **b** Co-immunoprecipitation of STAT3 and IP3R3. Whole-cell lysates or ER and MAM fractions were subjected to immunoprecipitation with anti-STAT3 antibodies (S3) or with control IgG, and blotted with the indicated antibodies. Representative of at least five independent experiments. *WCL* whole-cell lysate, *ER* endoplasmic reticulum, *MAM* mitochondrial-associated membranes, *T* total extract. **c** Whole-cell lysates from MDA-MB-468 cells were treated with the indicated amounts of Proteinase K (PK) in the presence or absence of 3% Triton-X 100 (Tx), and analysed by Western blot. Representative of five independent experiments

are the inositol 1,4,5-triphosphate receptors (IP3R), ligand-gated channels activated by the second messenger IP3, which is generated in response to many different extracellular signals [17]. While controlled Ca^{2+} release leads to the activation of mitochondria oxidative phosphorylation (OXPHOS) activity and ATP production, continuous or excessive release of Ca^{2+} leads to mitochondrial Ca^{2+} overload, the opening of the mitochondrial permeability transition pore, and the initiation of the intrinsic apoptotic program [18, 19]. Thus, regulation of the abundance and activity of the IP3Rs, and in particular of IP3R3, which is the main isoform expressed in most cultured cell lines [20] and is known to be preferentially involved in transmitting apoptotic Ca^{2+} signals to

mitochondria [21], plays a crucial role in determining the sensitivity of cells to apoptotic stimuli, in particular those acting via ER Ca^{2+} release, such as, for example, H_2O_2 and menadione [22]. Accordingly, several oncogenes and oncosuppressors, such as for example AKT, PTEN, and PML, have been shown to regulate IP3R3 activity and abundance, thus modulating sensitivity to apoptosis [22–25].

Here, we report the discovery that constitutively active STAT3 can regulate Ca^{2+} fluxes by localizing to the ER and MAMs and interacting with IP3R3, facilitating its degradation and enhancing cellular resistance to apoptotic stimuli. This appears to be a relevant mechanism in cancer, since STAT3 and IP3R3 levels are inversely correlated in basal-like mammary tumors, which often rely on constitutively active STAT3.

Results

STAT3 activity affects ER Ca^{2+} transfer and apoptotic responses

We have previously reported that constitutively active STAT3 causes a metabolic switch towards glycolysis, coupled to HIF-independent decreased mitochondrial activation as measured by mitochondrial Ca^{2+} uptake upon ATP stimulation [7]. Consistent with these findings, STAT3C MEF cells, which express a constitutively active STAT3 allele, displayed a statistically significant decrease in ER Ca^{2+} release when the cells were stimulated with ATP, an agonist that evokes a rapid discharge from inositol 1,4,5-phosphate receptors (IP3Rs) through interaction with G protein-coupled receptors, reflecting a slower flow of Ca^{2+} through the IP3R, as monitored by means of an ER-targeted Ca^{2+}-sensitive aequorin probe (Supplementary Fig. S1A, B). We thus decided to assess the role of STAT3 in regulating ER Ca^{2+} fluxes in human breast cancer cell lines, either displaying or not constitutive STAT3 activity (Supplementary Fig. S2). Strikingly, ER Ca^{2+} release was significantly increased upon inducible STAT3 silencing in MDA-MB-468 and MDA-MB-231 cells (Fig. 1a, b and Supplementary Fig. S1C, D), which display constitutive STAT3 phosphorylation on both Y705 and S727 (Supplementary Fig. S2) and are addicted to STAT3 activity. In contrast, STAT3 silencing did not affect ER Ca^{2+} release and content in the STAT3-independent MDA-MB-453 (Fig. 1c, d) and T47D (Supplementary Fig. S1F) cell lines, where STAT3 is not activated (Supplementary Fig. S2). Thus, similar to the STAT3C MEFs, constitutive STAT3 activity controls Ca^{2+} homeostasis at the ER compartment in STAT3-dependent breast cancer cells.

Oxidative stress can cause apoptosis by eliciting excessive Ca^{2+} release from the ER, which in turn triggers excessive Ca^{2+} intake into the mitochondria and the activation of the intrinsic apoptotic program [16]. In order to assess whether the alteration in ER Ca^{2+} release observed in the STAT3-dependent tumor cells upon STAT3 silencing correlates with altered apoptotic responses, we measured apoptosis in MDA-MB-468 cells, silenced or not for STAT3. Cells were treated with H_2O_2 or menadione, two oxidizing agents known to induce ER Ca^{2+} release and calcium-mediated cell death [22], and apoptosis was measured by means of Annexin V analysis (Fig. 1e). Interestingly, STAT3 silencing enhanced cell death in response to both H_2O_2 and menadione, but not to the genotoxic compound etoposide, whose mechanism of induced cell death is independent of Ca^{2+} [22]. Analogous results were obtained with MDA-MB-231 cells (Supplementary Fig. S1E). Accordingly, cytosolic Ca^{2+} concentration was significantly increased by treatment of STAT3-silenced MDA-MB-468 cells with H_2O_2 and menadione, but not etoposide (Fig. 1f–h). Consistently, neither apoptosis nor cytosolic Ca^{2+} was affected by STAT3 silencing in MDA-MB-453 or T47D cells (Fig. 1i–n and Supplementary Fig. S1G, H). Taken together, these results suggest that constitutively active STAT3 can reduce ER Ca^{2+} release upon oxidative stresses, thus inhibiting the apoptotic response.

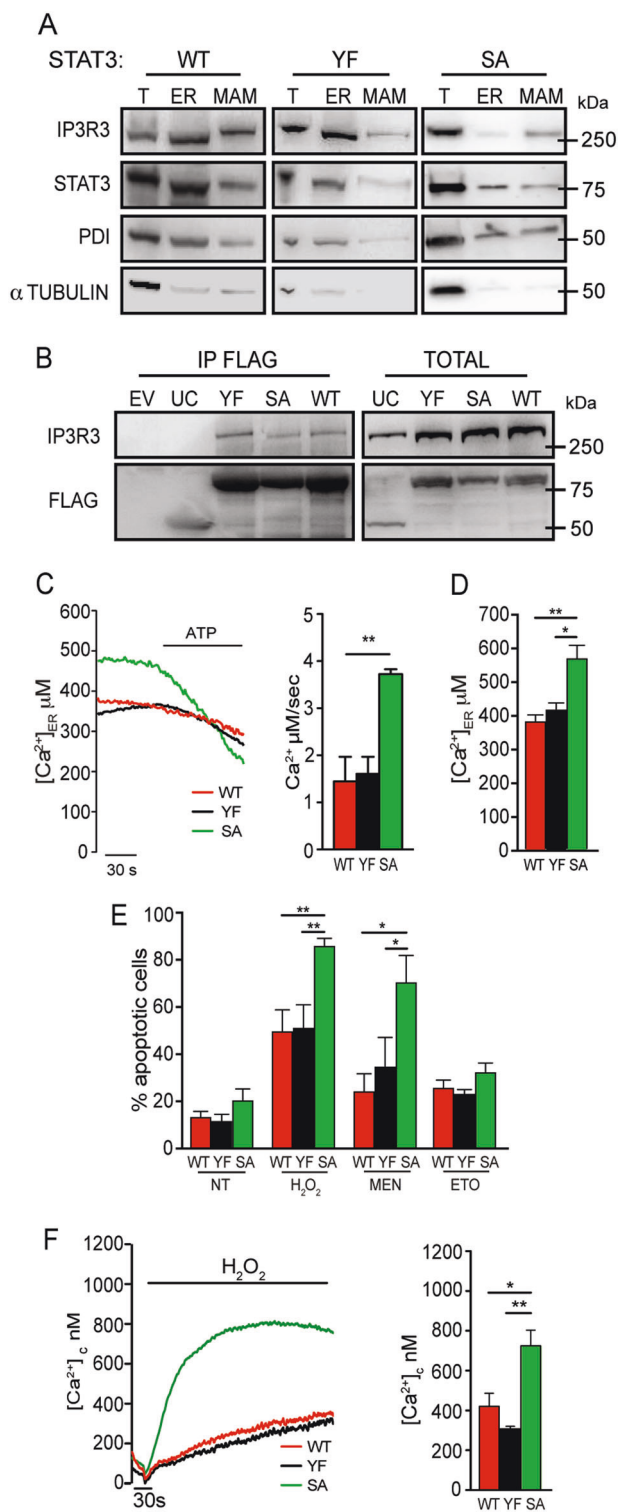## STAT3 localizes to the ER and MAM compartments, where it interacts with IP3R3

Since STAT3 was shown to localize to several cellular compartments including the mitochondrion [26], we assessed its subcellular localization in MDA-MB-468 cells. Strikingly, we observed that both the ER and the MAMs, the highly specialized ER compartment mediating communication with the mitochondrion, contained abundant STAT3, phosphorylated on both Y and S (Fig. 2a). A similar localization was also observed in primary MEFs and in the liver (Supplementary Fig. S3A, B). STAT3 was less abundant in the ER and MAMs of MDA-MB-453 and T47D breast tumor cells, where very little, if any, Y- or S-phosphorylated STAT3 was detected (Supplementary Fig. S3C, D). Thus, STAT3 may be responsible for regulating Ca^{2+} fluxes in response to apoptotic stimuli from within the ER and MAM compartments. In search for a possible mechanism, we assessed potential STAT3 interactions with known regulators of ER Ca^{2+} release, including the calcium channel IP3R3. Intriguingly, we observed a clear interaction of STAT3 with IP3R3, as evidenced by co-immunoprecipitation with anti-STAT3 antibodies (Fig. 2b). Of note, STAT3:IP3R3 interaction was detected not only in whole-cell extracts, but also in purified ER and MAM fractions of MDA-MB-468 cells, supporting the idea that the observed modulation of Ca^{2+} release is operated by ER- and MAM-localized STAT3. STAT3 and IP3R3 co-immunoprecipitated also from extracts of MDA-MB-453 cells (Supplementary Fig. S3E), despite their failure to display enhanced Ca^{2+} release or apoptosis upon STAT3 silencing. Thus, the mere interaction between STAT3 and IP3R3 is not sufficient to elicit a phenotype, strongly suggesting the involvement of differential phosphorylation instead. Importantly, the interaction was also detected using anti-IP3R3 antibodies in both cell types (Supplementary Fig. S3F).

Despite being an ER-transmembrane protein, most of IP3R3 faces the cytosolic side, where it has been shown to interact with several proteins, such as, for example, AKT, PML, and PTEN [22, 23]. In agreement with the idea that STAT3 may also interact with IP3R3 on the cytosolic side, both IP3R3 and STAT3 were eliminated from the ER fraction of MDA-MB-468 cells upon Proteinase K digestion, while the internal ER protein PDI was retained (Fig. 2c). As determined by co-IP experiments, both STAT3 coiled-coil and DNA-binding domains are involved in the interaction with IP3R3 (Supplementary Fig. S4A). Conversely, the N terminal domain of IP3R3, and more precisely the region between the residues 602 and 800, is engaged in the interaction with STAT3 (Supplementary Fig. S4B).

STAT3 S727 is involved in regulating Ca²⁺ release and apoptosis

In order to assess the role of STAT3 phosphorylation on either Y705 or S727 in regulating ER Ca^{2+} release and apoptosis, we reconstituted STAT3 null MEFs with FLAG-tagged STAT3, either wild type or mutated in the Y705 or the S727 residues (YF, SA). SA-mutated STAT3 is still detected in the ER and MAM fractions, albeit at a considerably reduced level as compared to the WT or YF forms, particularly in the MAMs (Fig. 3a). Likewise, all three STAT3 forms still co-immunoprecipitate with IP3R3 (Fig. 3b). These data suggest that phosphorylation on the Y or S residues is not absolutely required for either the ER/MAM localization or the interaction with IP3R3. Next, we investigated ER Ca^{2+} homeostasis. Interestingly, while MEFs expressing either the WT or the YF forms released comparable amounts of Ca^{2+} upon ATP stimulation, cells reconstituted with the SA form displayed significantly increased Ca^{2+} release, suggesting that phosphorylation on Serine 727 is involved in STAT3-mediated regulation of Ca^{2+} fluxes (Fig. 3c, d). This idea is confirmed by the observation that, compared with WT- or YF-reconstituted cells, MEFs reconstituted with SA-STAT3 displayed significantly enhanced apoptotic responses to H_2O_2 and menadione, but not to etoposide (Fig. 3e), similar to that

STAT3 activity regulates IP3R3 protein levels

Our data suggest that STAT3, by interacting with IP3R3, may regulate its ability to release Ca^{2+} in response to ATP, H_2O_2, or menadione. IP3R3 is known to be regulated at least partly via ubiquitination and proteasome degradation [25]. Interestingly, when analyzing the protein data available from CPTAC, the TCGA Cancer Proteome Study of Breast Tissue [27], we detected a negative correlation between STAT3 and IP3R3 protein levels (Fig. 4a, b). This was statistically significant within the basal-like breast cancer subtype, where STAT3 is often constitutively activated (Fig. 4b). In line with this observation, STAT3 silencing in the MDA-MB-468, but not in the MDA-MB-453, cells resulted in significant upregulation of IP3R3 protein levels (Fig. 4c, d), suggesting that indeed constitutively active STAT3 can control IP3R3 activity by downregulating its levels. We have recently reported that IP3R3 levels are significantly down-regulated upon serum starvation and re-feeding [25]. We thus wondered whether STAT3 activity might facilitate this degradation. Indeed, serum starvation/re-feeding resulted in significant downregulation of IP3R3 protein levels in MDA-MB-468 cells, strikingly correlating with a significant increase in the levels of serine-phosphorylated STAT3 (Fig. 4e and Supplementary Fig. S5C). This was dependent on proteasome activity and completely abolished by STAT3 silencing (Supplementary Fig. S5A and Fig. 4e). Of note, IP3R3 mRNA was not affected (Supplementary Fig. S5B). Intriguingly, expression of the STAT3-SA mutant in the silenced MDA-MB-468 cells failed to rescue IP3R3 degradation (Fig. 4e and Supplementary Fig. S5D). Taken together, these data suggest a link between S727 phosphorylation and the downregulation of IP3R3 levels, in keeping with the results obtained in MEFs. Further suggesting that IP3R3

observed in the MDA-MB-468 cells silenced for STAT3. Accordingly, SA-reconstituted MEFs displayed extremely higher levels of cytosolic calcium upon H_2O_2 treatment, as compared with the WT or YF cells (Fig. 3f), in agreement with a central role of S-P STAT3 in regulating ER Ca^{2+} release and apoptosis.
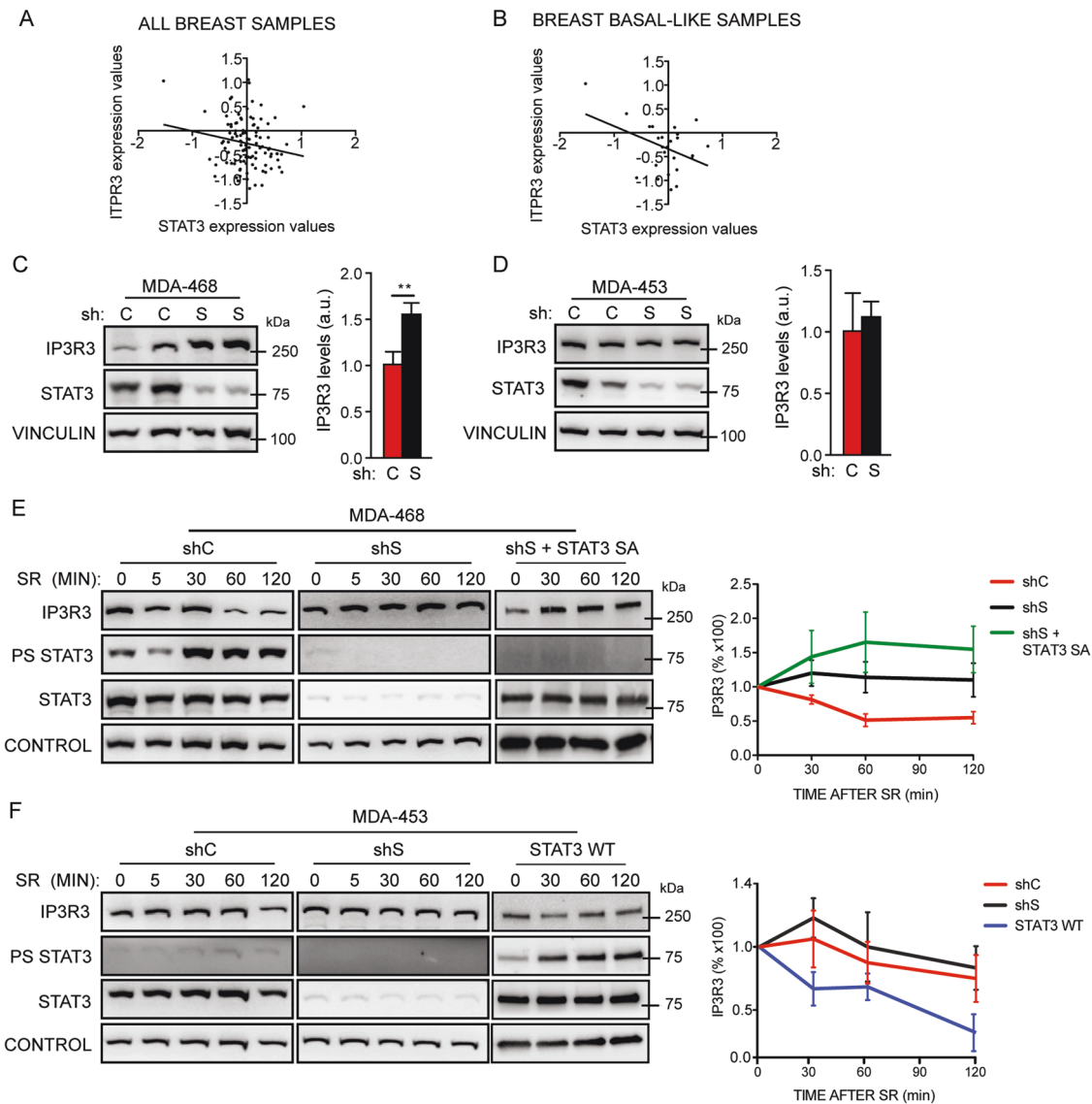
Fig. 4 STAT3-mediated regulation of IP3R3 protein levels in breast primary tumors and cell lines. **a, b** STAT3:IP3R3 anti-correlation in breast cancer patients from the CPTAC, TCGA Cancer Proteome Study of Breast Tissue dataset, considering all tumor subtypes (**a**, Pearson coefficient $= -0.18$, $P = 0.06$) or basal-like tumor samples (**b**, Pearson coefficient $= -0.41$, $P = 0.04$). **c, d** IP3R3 levels upon STAT3 silencing in MDA-MB-468 (**c**) or in MDA-MB-453 (**d**) cells. *shS* shSTAT3, *shC* sh control. Bars represent mean values ± SEM of four independent experiments. **e, f** IP3R3 levels upon starvation and serum restimulation (SR) in MDA-MB-468 (**e**) or MDA-MB-453 (**f**) cells silenced or not for STAT3 and overexpressing STAT3 SA or WT (shS, shSTAT3; shC, sh control). The graphs on the right show the relative quantification of IP3R3 levels from at least four independent experiments, as mean ± SEM. *P* values were calculated by two-way ANOVA. **e**, shC vs shS, $P < 0.001$; shC vs shS + STAT3 SA, $P < 0.001$; shS vs shS + STAT3 SA, ns. **f**, shC vs shS, ns; shC vs STAT3 WT, $P < 0.05$; shS vs STAT3 WT, $P < 0.01$

degradation requires STAT3 activity, no changes in IP3R3 expression were detected in MDA-MB-453 cells upon either STAT3 silencing or serum starvation and re-feeding, while the same cells overexpressing STAT3 underwent both STAT3 serine phosphorylation and IP3R3 degradation (Fig. 4f and Supplementary Fig. S5C, E). Of note, silencing of IP3R3 in MDA-MB-468 cells can recapitulate the effects of STAT3 activation on Ca^{2+} homeostasis (Supplementary Fig. S5 F, G), further supporting our conclusions.

Discussion

The regulation of calcium fluxes between the ER and mitochondria is crucial for the physiological and pathological regulation of energy metabolism and to inform cell decisions between energy production, and life, or apoptotic death. It is thus not surprising that the players involved in this equilibrium act as central signaling platforms for the activity of growth factors, oncogenes, and oncosuppressors

at the ER-mitochondria interface [16, 28]. For example, the activity of IP3R3 is regulated by a growing list of proteins that, mostly at MAMs, cooperate to modulate the activation of downstream pathways. Among them we would mention AKT, which destabilizes IP3R3 thus decreasing Ca^{2+} release and apoptosis, the stabilizing oncosuppressor PML [22], the anti-apoptotic Bcl-2 that inhibits Ca^{2+} transfer from ER to mitochondria by targeting IP3 receptors [29], and the chaperone Sig1R mainly involved in cell survival [30]. Noteworthy, recent findings highlighted the ability of the PTEN and BAP1 oncosuppressors to stabilize IP3R3 [23–25]. Accordingly, a wealth of data suggests a key role for this isoform in Ca^{2+} signaling and cell death [31–34].

STAT3 is a well recognized oncogene with potent anti-apoptotic functions, which have been linked both to its canonical nuclear activities, such as the direct regulation of anti-apoptotic genes transcription, and to its non-canonical functions exerted via localization to mitochondria, where it interacts with ETC components enhancing their activity while reducing ROS production, mediating RAS oncogenes-induced cell transformation [10, 12, 35]. Importantly, these non-canonical functions require STAT3 phosphorylation on S727 rather than on Y705. We have previously reported that constitutively active STAT3 enhances aerobic glycolysis, decreasing at the same time mitochondrial Ca^{2+} uptake, membrane polarization and OXPHOS activity, correlating with protection from apoptosis [7]. The mechanisms dictating these mitochondrial phenotypes are however still unclear. Here, we report that constitutively active STAT3 can reduce ER Ca^{2+} release. This correlates with resistance to apoptotic stimuli such as H_2O_2 and menadione, known to trigger Ca^{2+}-mediated cell death, but not to a Ca^{2+}-independent genotoxic stress such as etoposide [22]. Indeed, the STAT3-dependent MDA-MB-468 and MDA-MB-231 mammary tumor cells, which display constitutively active STAT3, become sensitive to Ca^{2+}-mediated cell death upon STAT3 silencing, while STAT3-independent MDA-MB-453 or T47D cells are not affected by the absence of STAT3. The observation that the enhanced sensitivity of MDA-MB-468 cells to apoptosis correlates with increased cytosolic Ca^{2+} in response to H_2O_2 and menadione in MDA-MB-468, but not in MDA-MB-453 cells, corroborates the idea that constitutively active STAT3 protects cells from specific apoptotic stimuli via the regulation of Ca^{2+} transfer from the ER. The further observation that STAT3, both phosphorylated on Y705 and on S727, localizes abundantly to the ER and the MAMs, where it interacts with IP3R3, provides a mechanistic explanation for this novel non-canonical activity of STAT3. In keeping with the previous knowledge about degradation-mediated IP3R3 regulation [16, 24, 25], we found that STAT3 silencing increases IP3R3 levels, and inhibits its degradation upon serum starvation and re-feeding in STAT3-dependent cells. These data suggest that constitutively active

STAT3 can promote IP3R3 degradation, thus reducing Ca^{2+} exit from the ER and apoptosis. It should be noted that some reports challenge the view of IP3R3 and Ca^{2+} fluxes to the mitochondria as part of the apoptotic machinery. For example, an increased expression of IP3R3 was noted in tumors [36, 37], where an efficient ER-mitochondrial Ca^{2+} transfer was proposed to ensure the activity of Ca^{2+}-dependent enzymes sustaining DNA synthesis and proliferation. Likewise, although reduced mitochondrial Ca^{2+} uptake was shown to allow cells to escape from apoptosis, Ca^{2+} fluxes towards mitochondria through the mitochondrial calcium uniporter appear to improve tumor growth and cell migration [38, 39]. Thus, like most metabolic parameters, also the role of Ca^{2+} signaling is likely continuously reshaped during the cell transformation route and under different conditions. Interestingly, phosphorylation on either Y705 or S727 is not strictly required for ER STAT3 localization, or for its interaction with IP3R3. However, our experiments with MEF cells reconstituted with tyrosine- or serine-mutated STAT3 clearly indicate that S727, but not Y705, is required for STAT3-mediated regulation of both ER Ca^{2+} fluxes and apoptosis. The additional observation that a STAT3 mutated on serine 727 fails to rescue the ability of STAT3-silenced MDA-MB-468 cells to undergo IP3R3 degradation upon serum starvation and re-feeding further supports the idea that SP-STAT3 regulates Ca^{2+} fluxes via controlling IP3R3 degradation. It can be speculated that serine phosphorylation, not required for STAT3-IP3R3 interaction, might be crucial for STAT3-mediated IP3R3 destabilization by either affecting its structure or recruiting some crucial component of the degradation complex. An alternative explanation is provided by the observation that the proportion of total STAT3 localizing to the ER is much lower not only in MEF cells reconstituted with the SA-STAT3 mutant as compared to those expressing either the WT or the YF mutant form, but also in the STAT3-independent MDA-MB-453 and T47D cells with respect to the STAT3-dependent MDA-MB-468 cells. This suggests the possibility that STAT3 phosphorylation on S727 facilitates STAT3 ER localization and function, which might become uninfluential below a certain threshold. Supporting the relevance of our findings is the observation that the levels of the two proteins are inversely correlated in basal-like breast cancer, where STAT3 constitutive activation plays a prominent role [40].

In the recent years, the pro-oncogenic role of S-P STAT3 has been demonstrated in many experimental systems, mostly linked to its functions in the mitochondrion [26]. However, the observation of very low molar ratios between mitochondrial STAT3 and ETC components has questioned the interpretation of a direct role of mitochondrial STAT3 in regulating ETC activities [41]. Besides the consideration that STAT3 abundance and role in the mitochondria is probably subjected to cell type and context variations, our

data suggest now an additional non-canonical, pro-oncogenic, and anti-apoptotic role exerted by constitutively phosphorylated STAT3 via its S727 residue.

Materials and methods

Cell lines, transfections, and animals

The breast cancer cell lines MDA-MB-468, MDA-MB-453, MDA-MB-231, and T47D were obtained from ATCC (Manassas, VA, USA) and expanded at the Molecular Biotechnology Center (MBC). Mice were maintained in the transgenic unit of the MBC in conformity with national and international laws and policies as approved by the Faculty Ethical Committee and by the Ministry of Health. Livers were collected from 8-week-old mice. Immortalized STAT3-null MEF cells were obtained as previously described [42]. Cell lines were grown in Dulbecco's modified Eagle medium (DMEM) with GLUTAMAX (Gibco-BRL, Carlsbad, CA, USA), supplemented with 10% (v/v) heat-inactivated FCS, 100 U/ml penicillin, and 100 µg/ml streptomycin (Gibco-BRL, Carlsbad, CA, USA). HEK293 cells were transiently transfected with pCDNA3 vectors carrying truncated forms of STAT3 and IP3R3 using Lipofectamine 2000 or Lipofectamine LTX systems (Life Technologies, Invitrogen, Carlsbad, CA, USA), according to manufacturer's instructions. STAT3 null MEF cells were transfected with pCEP4 vectors carrying WT or mutated (YF and SA) STAT3 forms, and stably expressing clones were selected with hygromycin.

Transduction with lentiviral vectors

Lentiviral viruses were packaged by transfecting 293T cells and used to infect cells for 24 h. For conditional RNA interference, the vectors pLV-DsRed-tTR-KRAB and the pLVTH-GFP-shRNA [43], either empty or carrying an shSTAT3 sequence as described [44], were produced. Cells were transduced at high efficiency with both lentiviral particles. Transduced cells were treated with doxycycline (1 µg/ml) for 12 h, followed by sorting of cells doubly positive for GFP and DsRed. STAT3 silencing was induced by 72 h doxycycline treatment (1 µg/ml). For the overexpression of STAT3, pLVX lentiviral vectors expressing either wild type or SA-STAT3, retromutated to make them sh-resistant, were used.

Calcium measurements

Cells were grown on glass coverslips at 50% confluence and ER Ca²⁺ measurements were performed as described [45]. Briefly, cells were infected with a lentiviral vector expressing the ER-aequorin chimera (ER-GFP-AEQm-pLV) for 48 h, then to reconstitute the probe with high efficiency, the luminal [Ca²⁺] of the ER was first reduced by incubating the cells for 45 min at 4 °C in Krebs–Ringer modified buffer (KRB; 125 mM NaCl, 5 mM KCl, 1 mM Na3PO4, 1 mM MgSO4, 5.5 mM glucose, and 20 mM 4-(2-hydroxyethyl)-1-piperazineethanesulfonic acid [HEPES], pH 7.4, at 37 °C) supplemented with 5 µM coelenterazine, the Ca²⁺ ionophore ionomycin, and 600 µM ethylene glycol tetraacetic acid (EGTA). After incubation, the cells were extensively washed with KRB supplemented with 2% bovine serum albumin and 2 mM EGTA before the luminescence measurement was initiated. Aequorin signals were measured in KRB supplemented with either 1 mM CaCl2 or 100 µM EGTA, using a purpose-built luminometer (see ref. [46] for complete details). The cytosolic Ca²⁺ response was evaluated essentially as described [47], making use of the fluorescent Ca²⁺ indicator Fura-2 AM (Life Technologies, Invitrogen). Briefly, cells were loaded with Fura-2 AM for 15 min, placed in an open Leyden chamber on a 37 °C thermostat controlled stage and treated with 1 mM H₂O₂. Fluorescence data at 340/380 nm were collected and expressed as calcium concentration (nM).

Detection of cell death

Cells were treated overnight with 1 mM H₂O₂, 15 µM menadione, or 150 M etoposide (Sigma Aldrich, St. Louis, MO, USA), followed by staining with Annexin V and Propidium Iodide according to manufacturer's protocol. Apoptosis was determined on a FACS Calibur cytometer (Beckton, Dickinson and Company, Franklin Lakes, NJ, USA).

Antibodies, Western blotting, and co-immunoprecipitations

Protein extracts were prepared with lysis buffer (150 mM NaCl, 50 mM Tris-HCl pH 7.4, 0.1% NP-40, 0.002M EDTA, 5% glycerol) supplemented with 1 mM PMSF and proteases/phosphatases inhibitors, fractionated on SDS-PAGE (4–12% precast gel, Life Technologies, Carlsbad, CA, USA) and transferred to a polyvinylidene difluoride membrane (Millipore, Billerica, MA, USA). Blots were probed using the following antibodies: mouse anti-IP3R-3 (cat. 610313, BD-Pharmingen, San Diego, CA, USA), rabbit anti-STAT3 (clone K15, cat. sc-483), rabbit anti-HA (cat. sc-805, Santa Cruz Biotechnologies, Dallas, Texas, USA), rabbit anti-PY (cat. 9131) and anti-PS STAT3 (cat. 9134), mouse anti-H3 (cat. 3638), rabbit anti-myc tag (cat. 2278, Cell Signaling, Danvers, MA, USA), mouse anti-PDI (cat. ab2792) and rabbit anti-VDAC1 (cat. ab15895, Abcam, Cambridge, UK), rabbit anti-SIGMAR1 (cat.

HPA018002), mouse anti-alphatubulin (cat. T5168), rabbit anti-FLAG (cat. F7425) and mouse anti-vinculin (cat. SAB4200080, Sigma Aldrich, St. Louis, MO, USA). Isotype matched, horseradish peroxidase-conjugated secondary antibodies were used followed by detection by chemiluminescence (Sigma Aldrich, St. Louis, MO, USA).

For co-immunoprecipitation experiments, freshly prepared pre-cleared lysates were incubated overnight at 4 °C with goat anti-IP3R3 (cat. sc-7277, Santa Cruz Biotechnologies, Dallas, Texas, USA) or rabbit anti-STAT3 (cat. 10253-2-AP, Proteintech, Rosemont, IL, USA) antibodies. Protein G or A beads, respectively (Ge Healthcare Bio-Science, Uppsala, Sweden), were added and rocked 2 h at 4 °C. Immunoprecipitations with anti-FLAG and anti-HA were performed by using ANTI-FLAG M2 Affinity Gel (cat. A2220) and Mouse Monoclonal Anti-HA-Agarose antibody (cat. A2095, Sigma Aldrich, St. Louis MO, USA) for 3 h at 4 °C. Immunoprecipitated proteins were boiled in 1x Laemmli buffer for 10 min prior to loading on SDS-PAGE.

Subcellular fractionations

Cells were fractionated as previously described [48]. Briefly, cells were harvested, washed in phosphate-buffered saline medium, resuspended in homogenization buffer, and gently disrupted by dounce homogenization. The homogenate was then submitted to different super- and ultra-centrifugation steps to obtain the indicated fractions.

Proteinase K digestion

The ER fraction was incubated with 50 µg/ml or 250 µg/ml of proteinase K for 30 min on ice, in the presence or not of 0.3% Triton-X 100. Samples were boiled in Laemmli buffer for 10 min prior to SDS-PAGE separation.

IP3R3 degradation assay

After silencing induction (see above), cells were serum-starved with 0.1% FCS in the presence of doxycyclin for 72 h, followed by FCS re-feeding in the presence of 100 M ATP (Sigma Aldrich, St. Louis, MO, USA). Samples were lysed and submitted to SDS-PAGE separation. For proteasome inhibition, two hours before re-feeding cells were treated with 40 µM MG132 (dissolved in dimethyl sulfoxide, DMSO), or with DMSO alone. IP3R3 levels were then detected by Western blot as described above.

RNA isolation and real-time PCR

Total RNA was extracted using Trizol reagent (Life Technologies, Invitrogen, Carlsbad, CA, USA) and used for cDNA synthesis with High Capacity Retrotranscription kit (Life Technologies, Applied Biosystems, Waltham, MA, USA). qRT-PCR reactions were performed using the Universal Probe Library system (Roche Italia, Monza, Italy). The 18S rRNA pre-developed TaqMan assay (Lifetech, Applied Biosystems, Waltham, MA, USA) was used as an internal control. Primer sequences were as follows: hIP3R3 L, 5′-tcgtgaagtatggcagtgtga-3′, hIP3R3 R, 5′-gaagccgcttgttcactgtc-3′ probe: 17.

Statistical analysis

Unpaired t test was used to calculate a P value for two groups. P values on a response affected by two factors were calculated with one-way or two-way ANOVA. P values are indicated as follows: $*P < 0.05$, $**P < 0.005$, $***P < 0.001$.

Compliance with ethical standards

Conflict of interest The authors declare that they have no conflict of interest.

References

1. Yu H, Lee H, Herrmann A, Buettner R, Jove R. Revisiting STAT3 signalling in cancer: new and unexpected biological functions. Nat Rev Cancer. 2014;14:736–46.
2. Yuan J, Zhang F, Niu R. Multiple regulation pathways and pivotal biological functions of STAT3 in cancer. Sci Rep. 2015;5:17663.
3. Pilati C, Amessou M, Bihl MP, Balabaud C, Nhieu JT, Paradis V, et al. Somatic mutations activating STAT3 in human inflammatory hepatocellular adenomas. J Exp Med. 2011;208:1359–66.
4. Waldmann TA. JAK/STAT pathway directed therapy of T-cell leukemia/lymphoma: inspired by functional and structural genomics. Mol Cell Endocrinol. 2017;451:66–70.
5. Bromberg JF, Horvath CM, Besser D, Lathem WW, Darnell JE Jr. Stat3 activation is required for cellular transformation by v-src. Mol Cell Biol. 1998;18:2553–8.
6. Avalle L, Regis G, Poli V. Universal and specific functions of Stat3 in solid tumors. In: Th. Decker MM (ed). *Jak-Stat Signaling: From Basics to Disease.* Springer-Verlag: Wien, 2012, pp 305–33.
7. Demaria M, Giorgi C, Lebiedzinska M, Esposito G, D'Angeli L, Bartoli A, et al. A STAT3-mediated metabolic switch is involved

in tumour transformation and STAT3 addiction. Aging. 2010;2:823–42.

8. Demaria M, Misale S, Giorgi C, Miano V, Camporeale A, Campisi J, et al. STAT3 can serve as a hit in the process of malignant transformation of primary cells. Cell Death Differ. 2012;19:1390–7.

9. Chung J, Uchida E, Grammer TC, Blenis J. STAT3 serine phosphorylation by ERK-dependent and -independent pathways negatively modulates its tyrosine phosphorylation. Mol Cell Biol. 1997;17:6508–16.

10. Gough DJ, Corlett A, Schlessinger K, Wegrzyn J, Larner AC, Levy DE. Mitochondrial STAT3 supports Ras-dependent oncogenic transformation. Science. 2009;324:1713–6.

11. Yokogami K, Wakisaka S, Avruch J, Reeves SA. Serine phosphorylation and maximal activation of STAT3 during CNTF signaling is mediated by the rapamycin target mTOR. Curr Biol. 2000;10:47–50.

12. Wegrzyn J, Potla R, Chwae YJ, Sepuri NB, Zhang Q, Koeck T, et al. Function of mitochondrial Stat3 in cellular respiration. Science. 2009;323:793–7.

13. Yang R, Lirussi D, Thornton TM, Jelley-Gibbs DM, Diehl SA, Case LK, et al. Mitochondrial Ca(2)(+) and membrane potential, an alternative pathway for Interleukin 6 to regulate CD4 cell effector function. eLife eLife 2015;4:e06376, 1–22.

14. Danese A, Patergnani S, Bonora M, Wieckowski MR, Previati M, Giorgi C, et al. Calcium regulates cell death in cancer: roles of the mitochondria and mitochondria-associated membranes (MAMs). Biochim Biophys Acta. 2017;1858:615–27.

15. Giorgi C, Missiroli S, Patergnani S, Duszynski J, Wieckowski MR, Pinton P. Mitochondria-associated membranes: composition, molecular mechanisms, and physiopathological implications. Antioxid Redox Signal. 2015;22:995–1019.

16. Marchi S, Patergnani S, Missiroli S, Morciano G, Rimessi A, Wieckowski MR, et al. Mitochondrial and endoplasmic reticulum calcium homeostasis and cell death. Cell Calcium 2018;69:62–72.

17. Mak DO, Foskett JK. Inositol 1,4,5-trisphosphate receptors in the endoplasmic reticulum: a single-channel point of view. Cell Calcium. 2015;58:67–78.

18. Bonora M, Morganti C, Morciano G, Pedriali G, Lebiedzinska-Arciszewska M, Aquila G, et al. Mitochondrial permeability transition involves dissociation of F1FO ATP synthase dimers and C-ring conformation. EMBO Rep. 2017;18:1077–89.

19. Morciano G, Giorgi C, Bonora M, Punzetti S, Pavasini R, Wieckowski MR, et al. Molecular identity of the mitochondrial permeability transition pore and its role in ischemia-reperfusion injury. J Mol Cell Cardiol. 2015;78:142–53.

20. Foskett JK, White C, Cheung KH, Mak DO. Inositol trisphosphate receptor Ca2+ release channels. Physiol Rev. 2007;87:593–658.

21. Mendes CC, Gomes DA, Thompson M, Souto NC, Goes TS, Goes AM, et al. The type III inositol 1,4,5-trisphosphate receptor preferentially transmits apoptotic Ca2+ signals into mitochondria. J Biol Chem. 2005;280:40892–40900.

22. Giorgi C, Ito K, Lin HK, Santangelo C, Wieckowski MR, Lebiedzinska M, et al. PML regulates apoptosis at endoplasmic reticulum by modulating calcium release. Science. 2010;330:1247–51.

23. Bononi A, Bonora M, Marchi S, Missiroli S, Poletti F, Giorgi C, et al. Identification of PTEN at the ER and MAMs and its regulation of Ca(2+) signaling and apoptosis in a protein phosphatase-dependent manner. Cell Death Differ. 2013;20:1631–43.

24. Bononi A, Giorgi C, Patergnani S, Larson D, Verbruggen K, Tanji M, et al. BAP1 regulates IP3R3-mediated Ca2+ flux to mitochondria suppressing cell transformation. Nature. 2017;546:549–53.

25. Kuchay S, Giorgi C, Simoneschi D, Pagan J, Missiroli S, Saraf A, et al. PTEN counteracts FBXL2 to promote IP3R3- and Ca2+ -mediated apoptosis limiting tumour growth. Nature. 2017;546:554–8.

26. Yang R, Rincon M. Mitochondrial Stat3, the need for design thinking. Int J Biol Sci. 2016;12:532–44.

27. Atlas N, Cancer Genome. Comprehensive molecular portraits of human breast tumours. Nature. 2012;490:61–70.

28. Bittremieux M, Parys JB, Pinton P, Bultynck GER. functions of oncogenes and tumor suppressors: modulators of intracellular Ca (2+) signaling. Biochim Biophys Acta. 2016;1863(6 Pt B):1364–78.

29. Rong YP, Bultynck G, Aromolaran AS, Zhong F, Parys JB, De Smedt H, et al. The BH4 domain of Bcl-2 inhibits ER calcium release and apoptosis by binding the regulatory and coupling domain of the IP3 receptor. Proc Natl Acad Sci USA. 2009;106:14397–402.

30. Hayashi T, Su TP. Sigma-1 receptor chaperones at the ER-mitochondrion interface regulate Ca(2+) signaling and cell survival. Cell. 2007;131:596–610.

31. Florea AM, Varghese E, McCallum JE, Mahgoub S, Helmy I, Varghese S, et al. Calcium-regulatory proteins as modulators of chemotherapy in human neuroblastoma. Oncotarget. 2017;8:22876–93.

32. Ivanova H, Vervliet T, Missiaen L, Parys JB, De Smedt H, Bultynck G. Inositol 1,4,5-trisphosphate receptor-isoform diversity in cell death and survival. Biochim Biophys Acta. 2014;1843:2164–83.

33. Mak DO, McBride S, Foskett JK. Regulation by Ca2+ and inositol 1,4,5-trisphosphate (InsP3) of single recombinant type 3 InsP3 receptor channels. Ca2+ activation uniquely distinguishes types 1 and 3 insp3 receptors. J Gen Physiol. 2001;117:435–46.

34. Hagar RE, Burgstahler AD, Nathanson MH, Ehrlich BE. Type III InsP3 receptor channel stays open in the presence of increased calcium. Nature. 1998;396:81–84.

35. Avalle L, Camporeale A, Camperi A. Poli V STAT3 in cancer: a double edged sword. Cytokine 2017;98:42–50.

36. Kang SS, Han KS, Ku BM, Lee YK, Hong J, Shin HY, et al. Caffeine-mediated inhibition of calcium release channel inositol 1,4,5-trisphosphate receptor subtype 3 blocks glioblastoma invasion and extends survival. Cancer Res. 2010;70:1173–83.

37. Mound A, Vautrin-Glabik A, Foulon A, Botia B, Hague F, Parys JB, et al. Downregulation of type 3 inositol (1,4,5)-trisphosphate receptor decreases breast cancer cell migration through an oscillatory Ca(2+) signal. Oncotarget. 2017;8:72324–41.

38. Tosatto A, Sommaggio R, Kummerow C, Bentham RB, Blacker TS, Berecz T, et al. The mitochondrial calcium uniporter regulates breast cancer progression via HIF-1alpha. EMBO Mol Med. 2016;8:569–85.

39. Gueguinou M, Crottes D, Chantome A, Rapetti-Mauss R, Potier-Cartereau M, Clarysse L, et al. The SigmaR1 chaperone drives breast and colorectal cancer cell migration by tuning SK3-dependent Ca(2+) homeostasis. Oncogene. 2017;36:3640–7.

40. Tell RW, Horvath CM. Bioinformatic analysis reveals a pattern of STAT3-associated gene expression specific to basal-like breast cancers in human tumors. Proc Natl Acad Sci USA. 2014;111:12787–92.

41. Phillips D, Reilley MJ, Aponte AM, Wang G, Boja E, Gucek M, et al. Stoichiometry of STAT3 and mitochondrial proteins: implications for the regulation of oxidative phosphorylation by protein-protein interactions. J Biol Chem. 2010;285:23532–6.

42. Schiavone D, Dewilde S, Vallania F, Turkson J, Di Cunto F, Poli V. The RhoU/Wrch1 Rho GTPase gene is a common transcriptional target of both the gp130/STAT3 and Wnt-1 pathways. Biochem J. 2009;421:283–92.

43. Wiznerowicz M, Trono D. Conditional suppression of cellular genes: lentivirus vector-mediated drug-inducible RNA interference. J Virol. 2003;77:8957–61.

44. Barbieri I, Quaglino E, Maritano D, Pannellini T, Riera L, Cavallo F, et al. Stat3 is required for anchorage-independent growth and metastasis but not for mammary tumor development downstream of the ErbB-2 oncogene. Mol Carcinog. 2010; 49:114–20.

45. Bonora M, Giorgi C, Bononi A, Marchi S, Patergnani S, Rimessi A, et al. Subcellular calcium measurements in mammalian cells using jellyfish photoprotein aequorin-based probes. Nat Protoc. 2013;8:2105–18.

46. Morciano G, Sarti AC, Marchi S, Missiroli S, Falzoni S, Raffaghello L, et al. Use of luciferase probes to measure ATP in living cells and animals. Nat Protoc. 2017;12:1542–62.

47. Patergnani S, Giorgi C, Maniero S, Missiroli S, Maniscalco P, Bononi I, et al. The endoplasmic reticulum mitochondrial calcium cross talk is downregulated in malignant pleural mesothelioma cells and plays a critical role in apoptosis inhibition. Oncotarget. 2015;6:23427–44.

48. Wieckowski MR, Giorgi C, Lebiedzinska M, Duszynski J, Pinton P. Isolation of mitochondria-associated membranes and mitochondria from animal tissues and cells. Nat Protoc. 2009;4:1582–90.